Estimating Radiation Interception in Heterogeneous Orchards Using High Spatial Resolution Airborne Imagery

M. L. Guillén-Climent, P. J. Zarco-Tejada, and F. J. Villalobos

***Abstract*—This letter outlines a method for quantifying the fraction of intercepted photosynthetically active radiation (fIPAR) from high spatial resolution airborne images acquired from an unmanned aerial vehicle. Airborne campaigns provided imagery of peach and citrus orchards using a six-band multispectral camera with 15-cm resolution. At the time of the airborne flights, field measurements of fIPAR taken with a ceptometer and structural data were obtained to characterize the study sites. Measuring fIPAR can be time consuming because of the need to sample for spatial and temporal variability. In this context, remote sensing techniques are useful as they make it possible to assess large areas. There is a lack of studies exploring the use of remote sensing techniques to estimate fIPAR in structurally complex crops. In this letter, the use of high spatial resolution imagery allowed us to classify each study plot into three pure components: vegetation, shaded soil, and sunlit soil. The radiation intercepted by a canopy is determined by the architecture and optical properties of the canopy. Consequently, the fractions of each component and their pure reflectance were used to estimate fIPAR in each study area with rmse $= 0.06$ for orange orchards and peach orchards.**

***Index Terms*—Fraction of intercepted photosynthetically active radiation (PAR) (IPAR) (fIPAR), orange, peach, remote sensing, row-structured orchards.**

I. Introduction

BIOMASS production and, therefore, crop yield are directly related to the ability of plants to convert absorbed solar radiation into dry matter [1], [2]. Absorbed photosynthetically active radiation (PAR) (APAR) sets a limit to potential production, which is determined by incident radiation and by the optical and architectural properties of the stand [3]. APAR takes into account both the incoming direct solar radiation and the PAR flux density reflected by the soil and the canopy [4], while intercepted PAR (IPAR) refers only to the ratio between PAR flux densities above and below the canopy. Since the difference between both is very small in full green canopies [5], we will consider the fraction of IPAR (fIPAR) as a proxy of the fraction of APAR in this study.

Field measurements and remote sensing retrieval are two approaches used to obtain accurate values of these parameters, which are widely used in agricultural applications [6]. Measuring IPAR and/or the related fIPAR can be time consuming because of the need to sample for spatial and temporal variability. In this context, remotely sensed data have considerable potential for providing information about the Earth's surface, as they make it possible to assess fIPAR in large areas. Exploring the within-field variability of fIPAR will help to optimize crop yield and production, which is one of the main targets of precision agriculture.

A literature review of the different methods—empirical and physical—used for remote sensing retrieval can be found in [4]. In this previous research, the use of the radiative transfer model contributed to the understanding of light interception by discontinuous canopies. In such canopies, which include those of fruit tree orchards, the fIPAR depends primarily on orchard architecture, which varies with the planting system, tree spacing, tree shape, tree height, alley width, row orientation, and leaf area index [7], [8]. The use of remote sensing to obtain maps showing the variability of fIPAR in an orchard is described in [4]. The normalized difference vegetation index (NDVI) has been found to be related to fIPAR in peach and orange orchards. This methodology is useful when high spatial resolution images are not available and it is not possible to obtain detailed information of the pure reflectance or the fraction of each component of the image. However, this previous research did not exploit the full potential of high spatial resolution imagery. Because of this, the purpose of this new study is to estimate fIPAR in row-structured orchards using the spatial detail obtained with high spatial resolution multispectral remote sensing imagery. The imagery acquired for this study allowed us to discriminate between vegetation, shaded soil, and sunlit soil components. Thus, it is possible to obtain the corresponding fractional areas and the pure reflectance of this type of complex canopy architecture. This approach exploits the spatial details of high-resolution data to determine fIPAR through scene component analysis.

Manuscript received October 30, 2012; revised April 26, 2013 and September 9, 2013; accepted September 25, 2013. Date of publication October 25, 2013; date of current version November 25, 2013. This work was supported in part by the Spanish Ministry of Science and Innovation (MCI) under Projects AGL2009-13105, CONSOLIDER CSD2006-67, and AGL2003-01463, by Junta de Andalucía under Excelencia AGR-595, and by Fondo Europeo de Desarrollo Regional.

M. L. Guillén-Climent and P. J. Zarco-Tejada are with the Instituto de Agricultura Sostenible, Consejo Superior de Investigaciones Científicas, 14080 Córdoba, Spain (e-mail: mariluzguillen@ias.csic.es; pablo.zarco@csic.es).

F. J. Villalobos is with the Departamento de Agronomía, Universidad de Córdoba, 14071 Córdoba, Spain (e-mail: ag1vimaf@uco.es).

Color versions of one or more of the figures in this paper are available online at http://ieeexplore.ieee.org.

Digital Object Identifier 10.1109/LGRS.2013.2284660

II. Materials and Methods

A. Study Area

The experimental fields were located in southern Spain. They included a 90-ha commercial peach orchard in Cordoba province (37° 48′ N, 4° 48′ W) and an 80-ha citrus orchard in Seville province (37° 20′ N, 5° 50′ W).

The study in the peach—*Prunus persica* (L.)—orchard was conducted with nectarine (cv. Sweet Lady) and peach (cv. Babygold) plantations. The nectarine and peach trees were planted at a spacing of 6 m × 3.3 m (500 trees · ha^{-1}) and 5 m × 3.3 m (600 trees · ha^{-1}), respectively, both with rows oriented 160° from the north (clockwise with north as zero). Eight plots were selected from this peach orchard. The study in the citrus plantation was conducted with sweet orange (*Citrus sinensis* L. Osb cv. Navelina) and clementine mandarin (*C. clementina* Hort. ex Tan. cv. Oronules) plantations. The orange and mandarin trees were planted at a spacing of 7 m × 3 m (476 trees · ha^{-1}) with rows in the east–west direction (70° from the north). Sixteen plots were selected from the citrus orchard. The study areas were selected to ensure spatial variability. They varied widely in vegetation cover fraction (4%–75% in citrus and 9%–60% in peach) and tree height (1.5–4 m) and had different row orientations between fields. The field campaigns were conducted in the summers of 2007 and 2008.

B. Ground and Airborne Remote Sensing Campaigns

The interception of PAR was measured with a ceptometer (SunScan Canopy Analysis System, Delta-T Devices Ltd., Cambridge, U.K.). The fraction of PAR intercepted by a tree is influenced by its surrounding trees and the background. Therefore, the area comprising the four central trees of each study plot was selected to conduct the field measurements of fIPAR (5 m × 3.3 m/6 m × 3.3 m for the peach orchard and 7 m × 3 m for the orange orchard). In each plot, the grids established to take the measurements with the ceptometer measured 1 m × 0.25 m. Between 66 and 84 measurements were taken depending on the area of the plot. As there was no understory, the measurements were acquired directly on the ground. Crown radius and tree height were measured with a scale pole. Details of the ceptometer measurements and the field measurements taken in the different study plots can be found in [4].

Field sampling and airborne overflights took place concurrently in these areas. Flights were conducted using an unmanned aerial vehicle (UAV) [9]–[11]. The camera consisted of six independent image sensors and optics with user-configurable spectral filters. The bands were centered at 490, 530, 570, 670, 700, and 800 nm. Bands belonging to the PAR region (400–700 nm) were used in this study. The imagery had 15-cm pixel spatial resolution at 150-m flight altitude. Atmospheric correction and radiometric calibration methods were applied to the imagery to calculate spectral reflectance. Radiometric calibration was conducted in the laboratory using coefficients derived from measurements taken with a uniform calibration body. Radiance values were converted to reflectance using the total incoming irradiance simulated with the Simple Model of Atmospheric Radiative Transfer of Sunshine (SMARTS) [12]. More details about reflectance obtained from UAV imagery, validation, and camera specifications can be found in [4].

The measurements of the spatial variation of fIPAR in different plots were conducted at 10:00 GMT (± half-hour). Additionally, measurements of fIPAR and multispectral imagery were obtained at different times of the day in two plots—one from each orchard—for diurnal variability studies (09:00, 10:00, and 11:00 GMT).

C. fIPAR Estimation

The high spatial resolution imagery was analyzed to obtain the percentage and reflectance of each component of the scene—vegetation, shaded soil, and sunlit soil. A detailed quantification of the optical properties of the soil and vegetation was obtained with this methodology in each plot. Therefore, the optical properties were not assumed to be constant within each orchard. Soil variability and vegetation variability were taken into account in the entire study area. These parameters were then used to estimate instantaneous fIPAR. The factors that determine the intercepted radiation regime in vegetation canopies are the architecture of the canopy, the optical properties of vegetation elements and the soil, and the spectral composition of the incident radiation field [13]. The fIPAR for each plot was calculated as

$$\begin{aligned} \text{fIPAR} &= (\text{fr}_v + \text{fr}_{\text{shsfa}}) \cdot (1 - \tau_p) \\ &= \text{fr}_{\text{shs}} \cdot \left(1 - \frac{\text{rfl}_{\text{PARshs}}}{\text{rfl}_{\text{PARss}}}\right) \end{aligned} \tag{1}$$

where fr_v is the fraction of vegetation, fr_{shsfa} is the fraction of shaded soil seen from above, and τ_p is the vegetation transmissivity in the PAR region (400–700 nm), computed as one minus the reflectance of shaded soil $(\text{rfl}_{\text{PARshs}})$ divided by the reflectance of sunlit soil $(\text{rfl}_{\text{PARss}})$. Reflectance was computed as the mean of the reflectances obtained in the PAR region. The fractions of shaded and sunlit soil due to the solar direction (related to fIPAR) are the same as the fractions viewed from the airborne platform. Yet, a limitation related to this methodology is that the nadir view does not allow discriminating the fraction of shaded soil directly under the vegetation. The omission of the unexposed area below the vegetation may lead to an underestimation of fIPAR. Therefore, an alternative method was used to estimate the fraction of shaded soil: A distinction was made between shaded soil visible from above and shaded soil hidden by vegetation cover; fr_{shs} was computed as the sum of the fraction of shaded soil seen from above plus the fraction of vegetation.

The ratio between reflectance from shaded soil and reflectance from sunlit soil represents the fraction of solar radiation that has passed through the canopy. The main assumptions of the model are the following: 1) The scattered PAR that reaches the soil surface is negligible; 2) the soil below the vegetation is fully shaded; and 3) the transmittance of PAR within the shaded areas is constant.

Each plot was classified into three components—vegetation, shaded soil, and sunlit soil [Fig. 1(a)]—using a supervised classification methodology. The *Mahalanobis distance* supervised classification [14] was used to obtain the classified image of

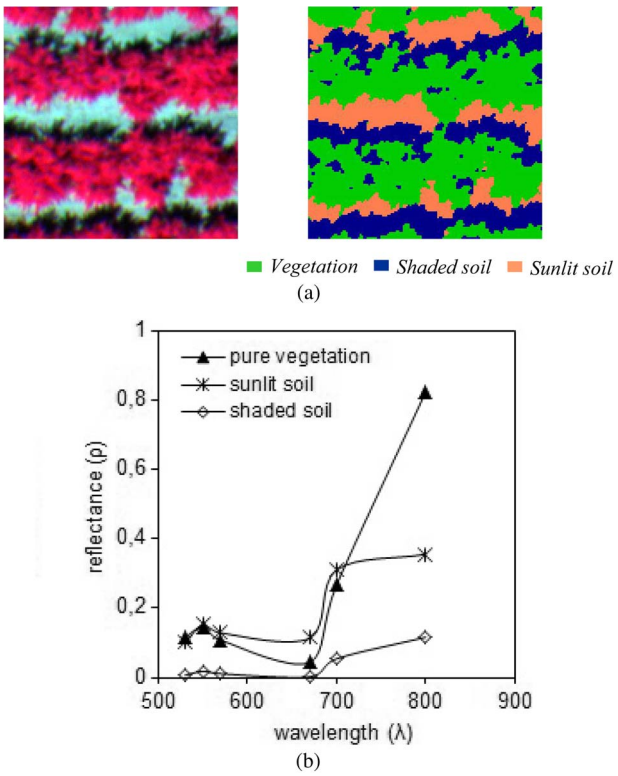

Fig. 1. Multispectral reflectance images of the peach orchard acquired at 10-nm full-width at half-maximum (FWHM) and 15-cm spatial resolution, showing (a) one of the plots and (b) the reflectance of each component from the classified image.

the different study plots. Five regions of interest comprising 20 pure pixels were manually selected for each component of the image to train the *Mahalanobis distance* algorithm. After the classification, some misclassifications were corrected by converting shaded soil patches into vegetation patches when they were surrounded by vegetation.

III. Results

A. Imagery Classification

The *Mahalanobis distance* supervised classification yielded errors ranging between 0.8% and 3% for the fraction of vegetation.

In order to assess classification consistency, a comparison was made between the vegetation cover fractions obtained in two selected plots at the different times of the day in a diurnal study. In the plots where diurnal studies were carried out, the mean vegetation fraction was obtained from the image classification at 9:00, 10:00, and 11:00 GMT. Errors were computed by comparing the mean vegetation fraction with the values obtained at each time. Fig. 2 shows a plot of the orange orchard at 9:00 GMT [Fig. 2(a) and (b)], 10:00 GMT [Fig. 2(c) and (d)], and 11:00 GMT [Fig. 2(e) and (f)].

B. Estimating fIPAR Using High Spatial Resolution Imagery Classification

The estimated fIPAR obtained from the application of the algorithm [1] was compared to the value obtained in the field

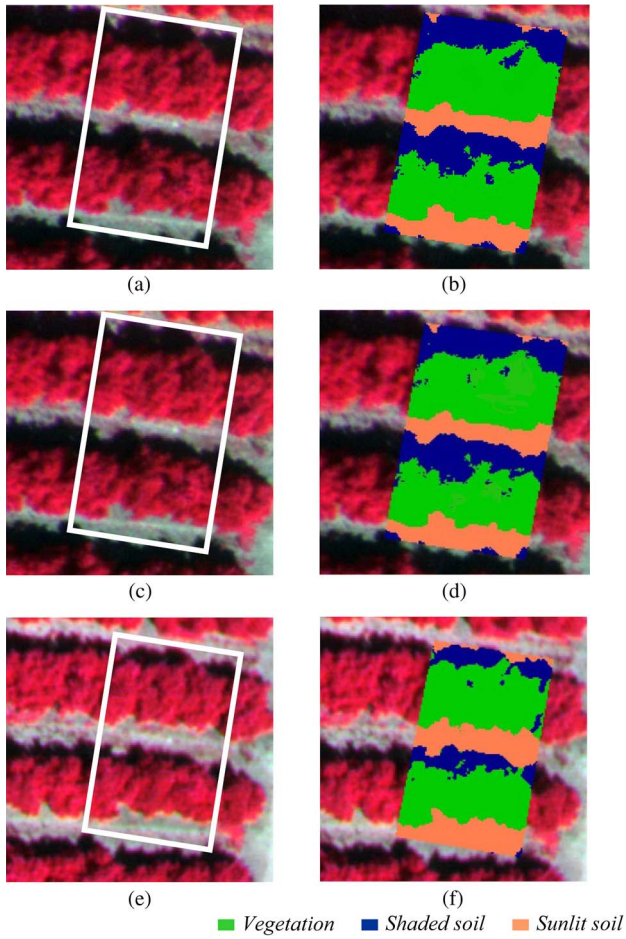

Fig. 2. [(a), (c), and (e), respectively] Diurnal evolution of the shadows in an orange study plot at 9:00, 10:00, and 11:00 GMT and [(b), (d), and (f)] classified images obtained.

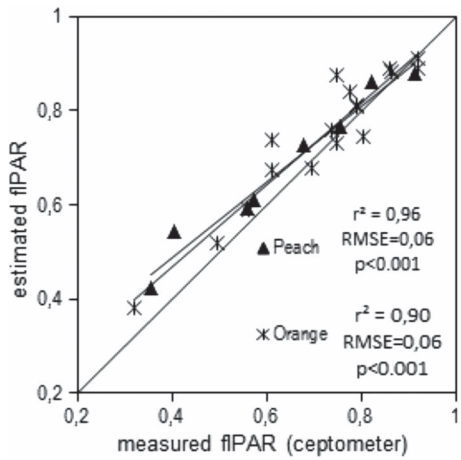

Fig. 3. Estimated intercepted radiation using high spatial resolution analysis versus measured fIPAR.

using the ceptometer. The assessment yielded rmse values of 0.06 for orange and peach plots (Fig. 3). In the youngest trees (Fig. 4), where the crowns were less overlapped than in more mature trees, the fraction of shadow under the tree was smaller, and the error increased. Thus, it was assumed that the largest errors came from the unknown fraction of shaded soil under the crown. Nonetheless, these results are slightly better than

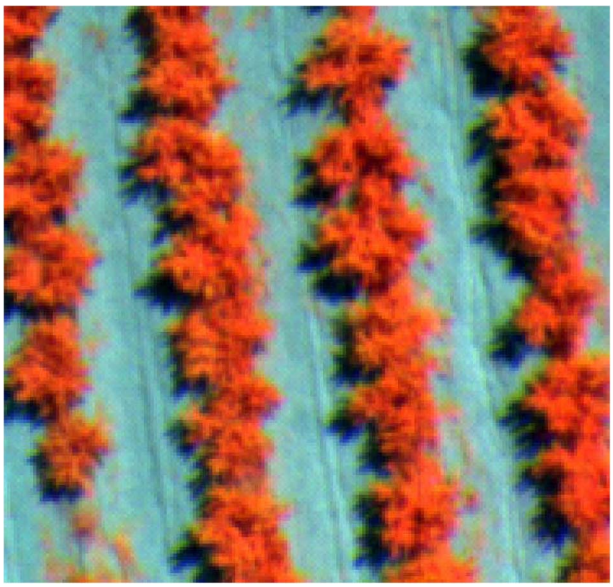

Fig. 4. Airborne multispectral image of young peach trees obtained at 15-cm resolution and 10-nm FWHM spectral bandwidth.

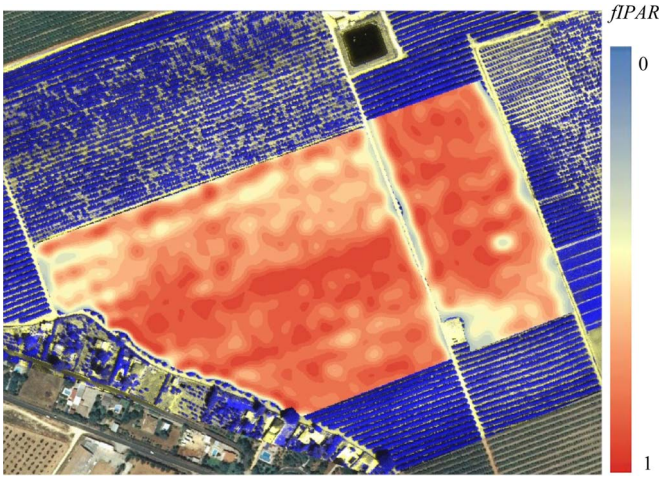

Fig. 5. Map of fIPAR calculated from high spatial resolution imagery and multispectral mosaic of the citrus orchard acquired from the UAV platform (the real color parts are outside the study area).

those obtained previously in [4], where aggregated pixels were used to compute the spectral vegetation index obtained from multispectral imagery and related to fIPAR. In that previous study, an r^2 of 0.85 and an rmse of 0.9 were obtained. The currently proposed methodology ignores the actual contribution of diffuse radiation below the canopy to the estimation of the reference soil irradiance used to derive the transmissivity of trees. The error is likely to be small considering the low rmse observed. In addition, this contribution should be large only when fIPAR is high (and transmissivity is low). Thus, the combined effect should be small.

A direct application of these techniques made it possible to map the spatial variation of fIPAR at the orchard scale using very high resolution airborne imagery (Fig. 5). The figure shows the mosaic obtained with the remotely sensed data for the orange orchard. A part of the map showing the spatial variability of fIPAR in the orange orchard is overlapped on this mosaic. The sensitivity of estimated productivity to fIPAR will depend on radiation use efficiency (RUE) for fruit production as defined in [15]. For instance, Whitney and Wheaton [16] reported yields of 62 t/ha for orange trees with a seasonal fIPAR of 0.67 in Florida, which implies an average RUE of 3.2 g fruit/(MJ PAR). Therefore, the rmse of yield would be 5.5 t/ha.

IV. Conclusion

A methodology for analyzing high spatial resolution multispectral imagery of heterogeneous crop canopies such as peach and citrus orchards has been proposed. The imagery was classified into pure components of vegetation, shaded soil, and sunlit soil using the 15-cm multispectral imagery acquired from a UAV. Pure reflectance and the fractions of the various components were used to estimate fIPAR. A supervised classification was found to be successful in distinguishing the different components.

Estimates of fIPAR yielded an rmse of 0.06 for orange and peach plantations. These estimations are more accurate than those obtained using previous methodology when aggregated NDVI is used to estimate fIPAR [4] if high spatial resolution is available. In addition, this method does not rely on empirical determinations between fIPAR and parameters based on reflectance. Instead, it is based on measuring the actual components of radiation interception. Potential errors may arise from ignoring the actual contribution of diffuse radiation below the canopy and the overlap of vegetation and shade as seen from above. This issue deserves further research.

The two methodologies that use medium spatial resolution imagery [4] and this new method based on detailed information obtained from very high spatial resolution imagery make it possible to obtain maps showing the spatial variability of fIPAR in orchards. However, information about soil optical properties improves the estimation of fIPAR when scene components can be quantified using very high resolution imagery. This methodology will make it possible to map fIPAR and, therefore, the potential productivity of fruit tree orchards. Studies using this methodology in vineyards are currently being conducted, which will provide a wider data set of field measurements. Diurnal studies will be used to explore the variability and uncertainties associated with this methodology. In addition, the estimation of daily PAR interception from estimated instantaneous fIPAR in these complex canopies should also be studied.

Acknowledgment

The authors would like to thank the members of the QuantaLab, Instituto de Agricultura Sostenible, Consejo Superior de Investigaciones Científicas, for the scientific and technical support in field and airborne campaigns.

References

[1] M. Monsi and T. Saeki, "Uber den liechfaktor in den pflanzengesellschaften und seine bedeutung für die stoffproduktion (*On the factor light in plant communities and its importance for matter production*)," *Jpn. J. Bot.*, vol. 14, pp. 22–52, 1953.

[2] J. L. Monteith, "Solar radiation and productivity in tropical ecosystems," *J. Appl. Ecol.*, vol. 9, no. 3, pp. 747–766, Dec. 1972.

[3] J. Ross, *The Radiation Regime and Architecture of Plant Stands*. Hague, The Netherlands: W. Junk, 1981.
[4] M. L. Guillén-Climent, P. J. Zarco-Tejada, J. A. J. Berni, P. R. J. North, and F. J. Villalobos, "Mapping radiation interception in row-structured orchards using 3D simulation and high resolution airborne imagery acquired from a UAV," *Precis. Agr.*, vol. 13, no. 4, pp. 473–500, Aug. 2012.
[5] C. S. T. Daughtry, K. P. Gallo, S. N. Goward, S. D. Prince, and W. P. Kustas, "Spectral estimates of absorbed radiation and phytomass production in corn and soybean canopies," *Remote Sens. Environ.*, vol. 39, no. 2, pp. 141–152, Feb. 1992.
[6] S. Liang, X. Li, and J. Wang, "Advanced remote sensing," in *Terrestrial Information Extraction and Applications*. Amsterdam, The Netherlands: Elsevier, 2012, p. 800.
[7] J. E. Jackson, "Light interception and utilization by orchard systems," *Horticult. Rev.*, vol. 2, pp. 208–267, 1980.
[8] T. Robinson and A. Lakso, "Bases of yield and production efficiency in apple orchard system," *J. Amer. Soc. Horticult. Sci.*, vol. 116, no. 2, pp. 188–194, Mar. 1991.
[9] J. A. J. Berni, P. J. Zarco-Tejada, L. Suarez, and E. Fereres, "Thermal and narrow-band multispectral remote sensing for vegetation monitoring from an unmanned aerial vehicle," *IEEE Trans. Geosci. Remote Sens.*, vol. 47, no. 3, pp. 722–738, Mar. 2009.
[10] P. J. Zarco-Tejada, J. A. J. Berni, L. Suárez, and E. Fereres, "A new era in remote sensing of crops with unmanned robots," in *Proc. SPIE Newsroom*, 2008, pp. 2–4.
[11] P. J. Zarco-Tejada, V. González-Dugo, and J. A. J. Berni, "Fluorescence, temperature and narrow-band indices acquired from a UAV platform for water stress detection using a micro-hyperspectral imager and a thermal camera," *Remote Sens. Environ.*, vol. 117, pp. 322–337, Feb. 2012.
[12] C. A. Gueymard, "Interdisciplinary applications of a versatile spectral solar irradiance model: A review," *Energy*, vol. 30, no. 9, pp. 1551–1576, Jul. 2005.
[13] Y. Wang, W. Buermann, P. Stenbergb, H. Smolander, T. Häme, Y. Tian, J. Hu, Y. Knyazikhin, and R. Myneni, "A new parameterization of canopy spectral response to incident solar radiation: Case study with hyperspectral data from pine dominant forest," *Remote Sens. Environ.*, vol. 85, no. 3, pp. 304–315, May 2003.
[14] J. A. Richards, *Remote Sensing Digital Image Analysis*. Berlin, Germany: Springer-Verlag, 1999.
[15] F. J. Villalobos, L. Testi, J. Hidalgo, M. Pastor, and F. Orgaz, "Modelling potential growth and yield olive (*Olea europaea* L.) canopies," *Eur. J. Agr.*, vol. 24, no. 4, pp. 296–303, May 2006.
[16] J. D. Whitney and T. A. Wheaton, "Tree spacing affects citrus fruit distribution and yield," in *Proc. Florida State Horticul. Soc.*, 1984, vol. 97, pp. 44–47.